

Supporting Information

Laser Direct Writing-Electrochemical Anodizing Composite Manufacturing Biomimetic Superwetting Multifunctional Surfaces

Pengcheng Yan¹, Yuanyuan Hou^{1*}, Naizhen Sun¹, Mengran Yu¹, Yongling Wu¹, Mingming Liu^{1,2*}, Hongyu Zheng^{1*}

¹School of Mechanical Engineering, Shandong University of Technology, Zibo 255000, China.

² State Key Laboratory of Solid Lubrication, Lanzhou Institute of Chemical Physics, Chinese Academy of Sciences, Lanzhou 730000, P. R. China.

*Corresponding authors: houyuanyuan1990@126.com, mmliu_1221@hotmail.com, zhenghongyu@sdu.edu.cn

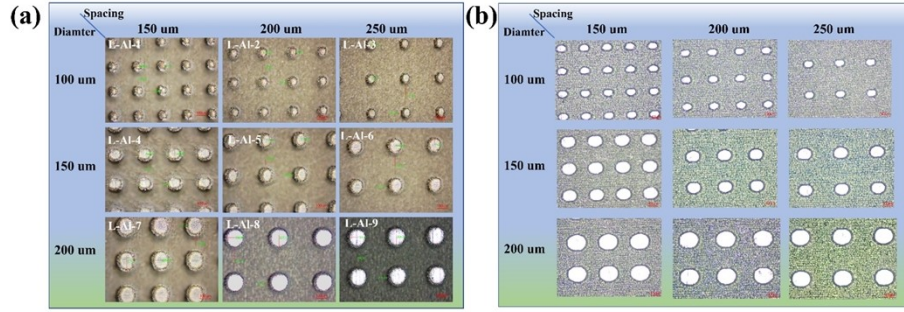


Fig.S1 Optical microscopy diagrams of (a) L-Al and (b) L-AAO with different structural parameters.

TableS1: Naming of samples with different structural parameters

Sample	Sample	Sample	Diameter/ um	Spacing/um
L-Al-1	L-AAO-1	L-AAO@PFOTS-1	100	150
L-Al-2	L-AAO-2	L-AAO@PFOTS -2	100	200
L-Al-3	L-AAO-3	L-AAO@PFOTS -3	100	250
L-Al-4	L-AAO-4	L-AAO@PFOTS -4	150	150
L-Al-5	L-AAO-5	L-AAO@PFOTS -5	150	200
L-Al-6	L-AAO-6	L-AAO@PFOTS -6	150	250
L-Al-7	L-AAO-7	L-AAO@PFOTS -7	200	150
(L-Al)	(L-AAO)	(L-AAO@PFOTS)		
L-Al-8	L-AAO-8	L-AAO@PFOTS -8	200	200
L-Al-9	L-AAO-9	L-AAO@PFOTS -9	200	250

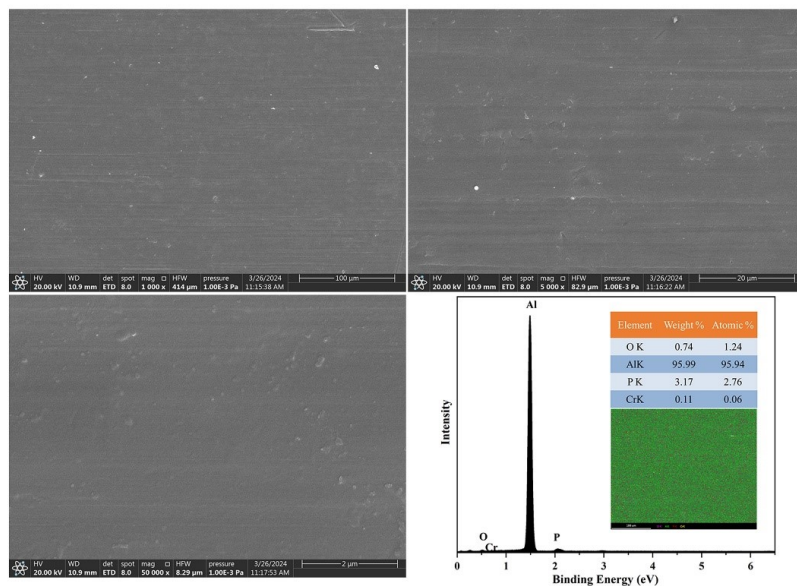


Fig.S2 EDS of Al

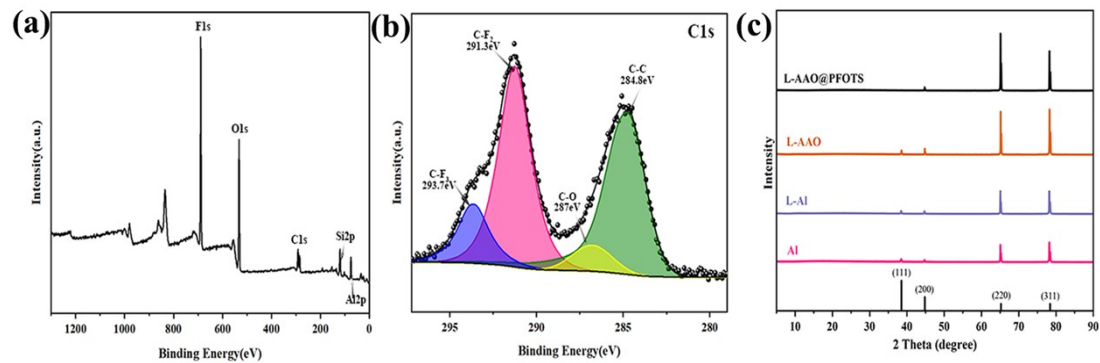


Fig.S3. (a) XPS spectra of (a) full spectrum, (b) C1s and (c) XRD of Al、L-Al
L-AAO、L-AAO@PFOTS

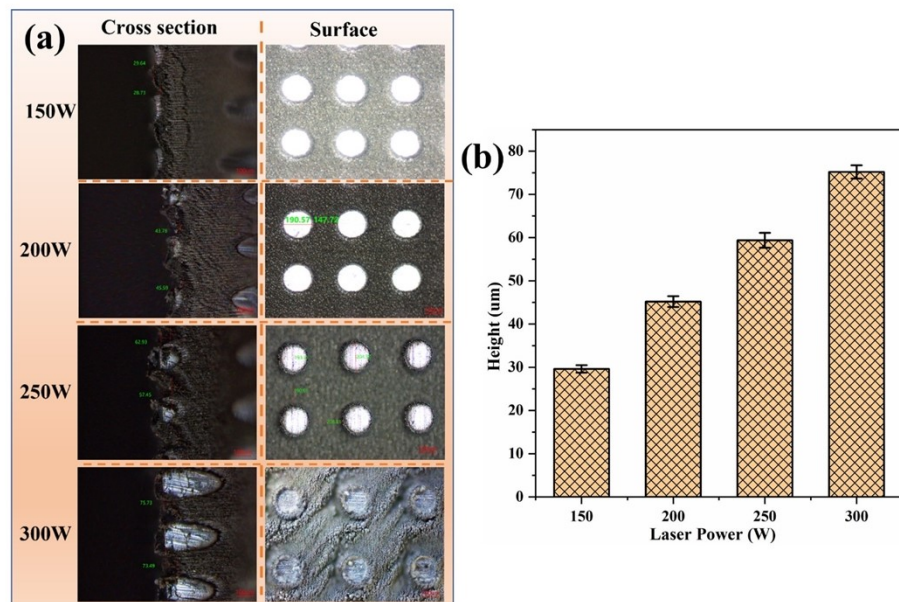


Fig.S4. Effect of different laser powers on (a) surface morphology, (b) Structural depth.

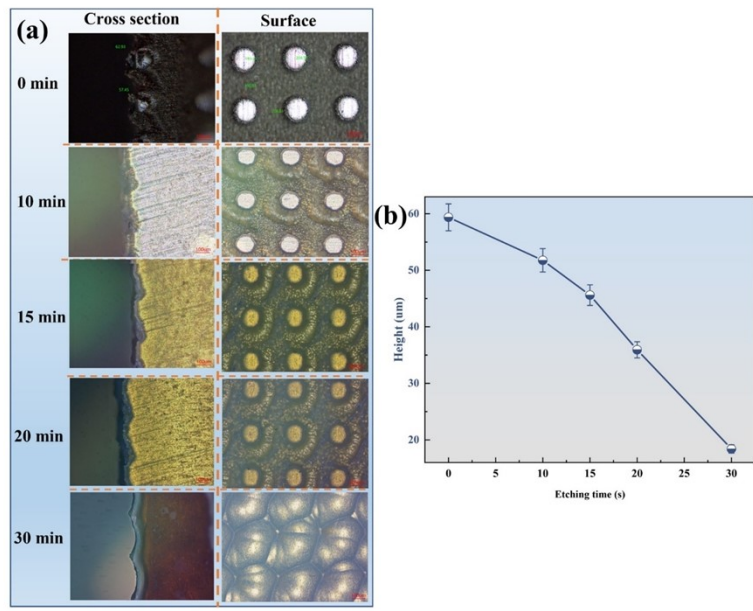


Fig.S5 Effect of anodization time on (a) the surface morphology and (b) structural depth of L-AAO

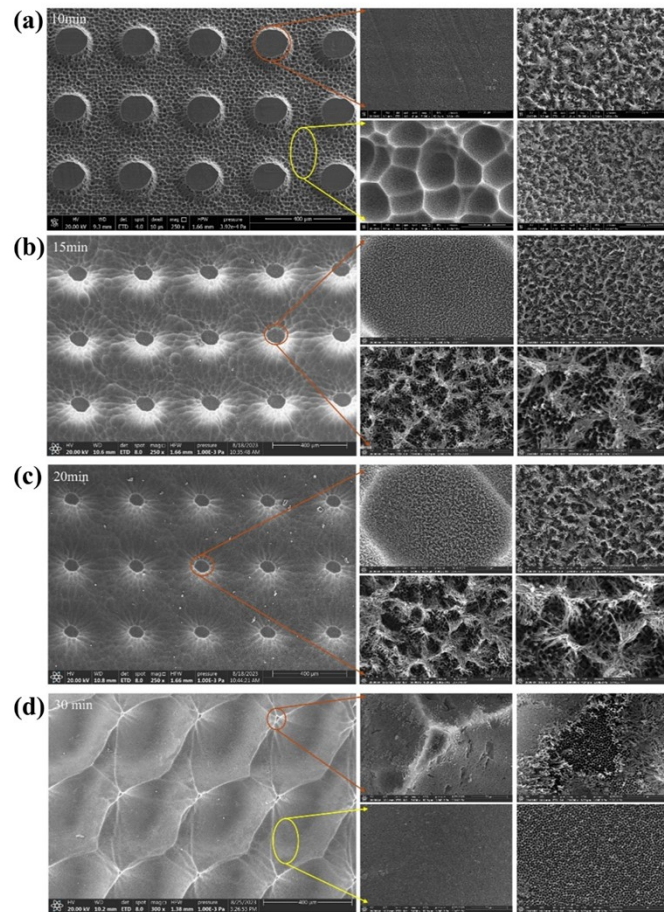


Fig.S6. SEM of different anodization times on the surface morphology of L-AAO.(a)10min,(b)15min,(c)20min,(d)30min.

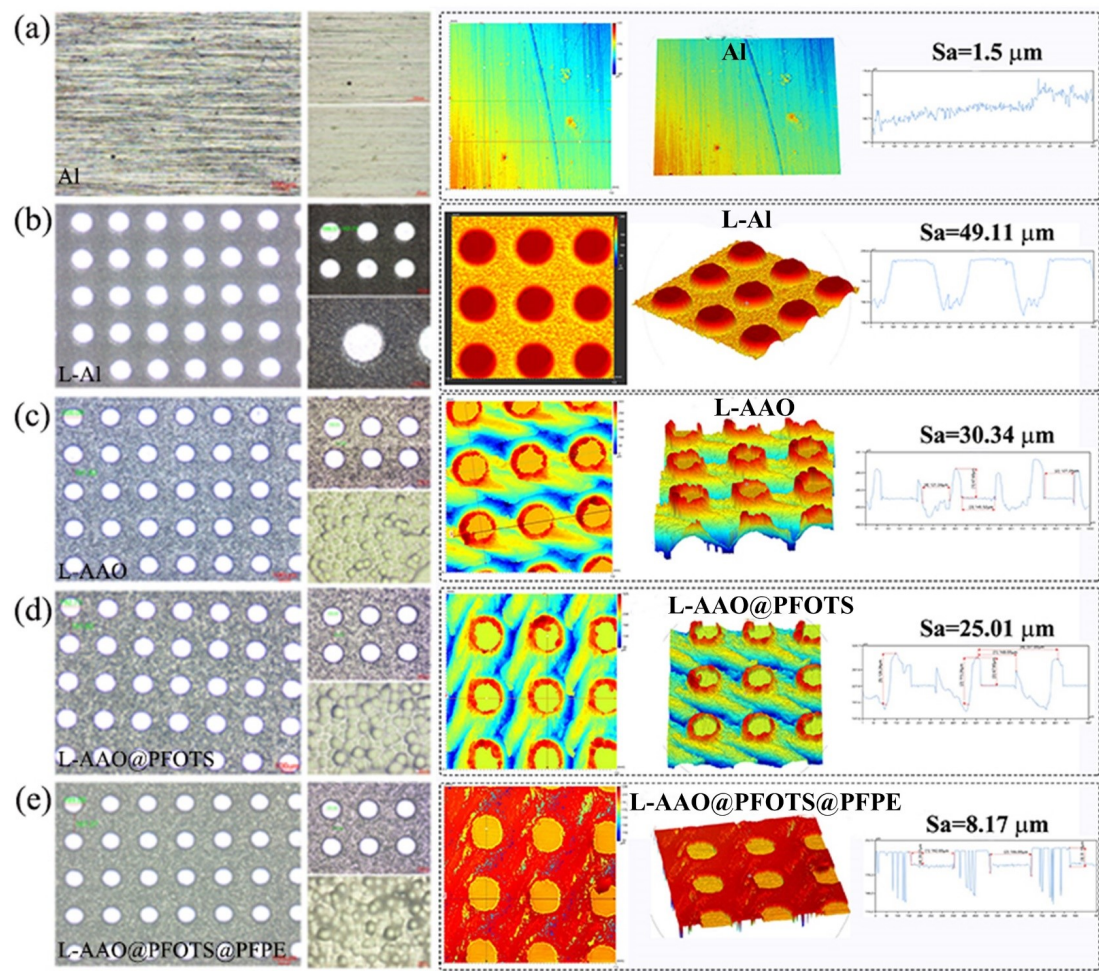


Fig.S7.Optical microscope images and 3D confocal microscope images of Al, L-Al, L-AAO, L-AAO@PFOTS, and L-AAO@PFOTS@PFPE.

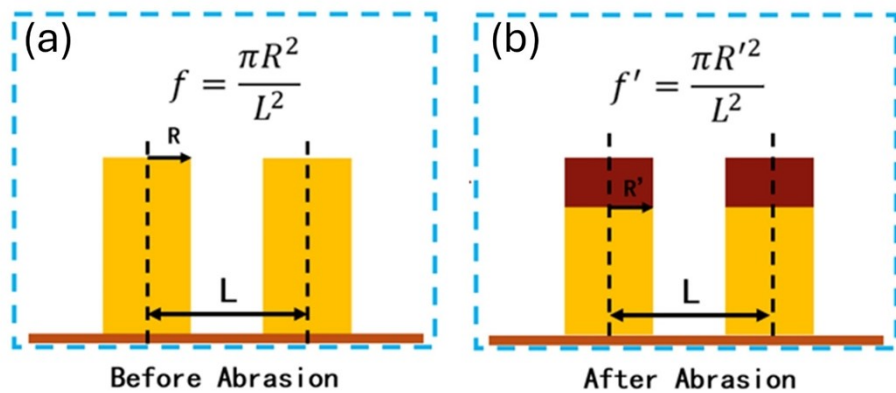


Fig.S8. The schematic diagram of the micro-pillars structure before and after friction.

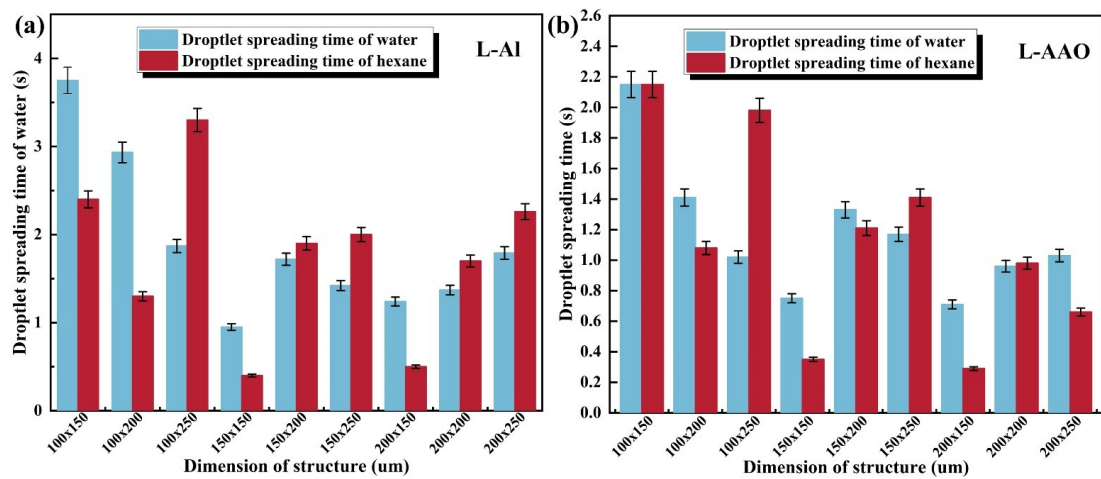


Fig.S9. The droplet spreading time of water and n-hexane on (a) L-Al and (b) L-AAO surfaces with different structural parameters.

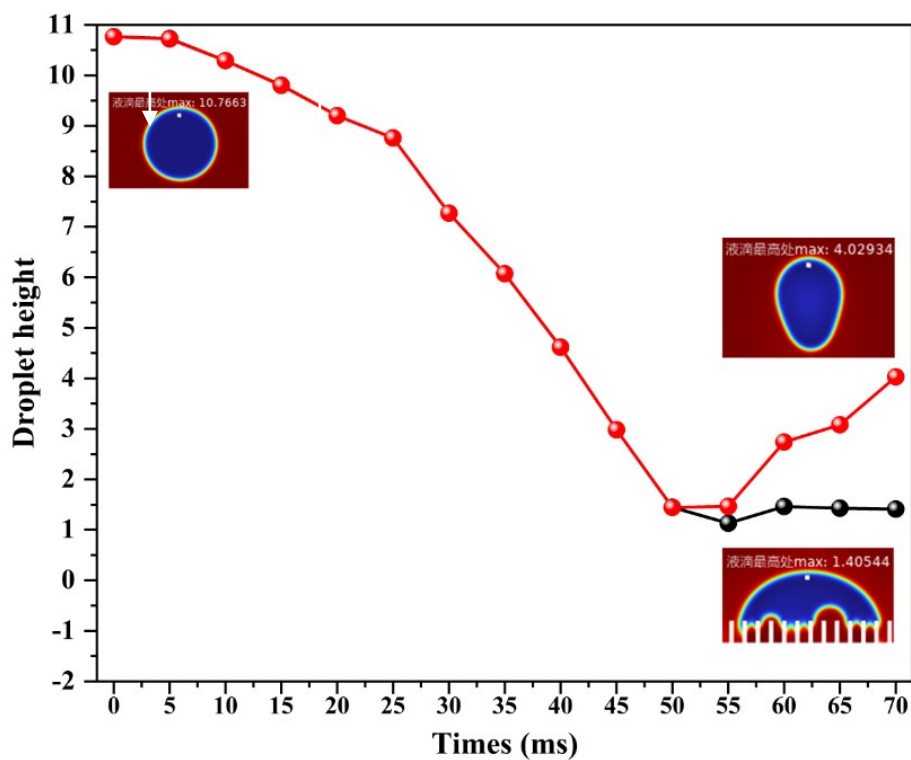
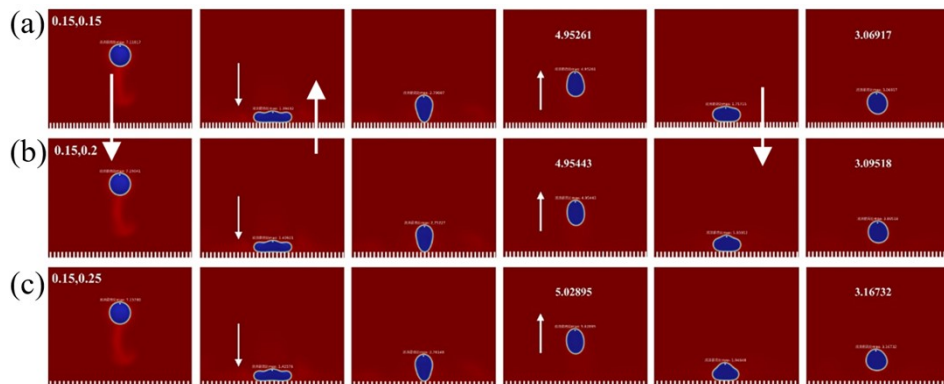


Fig.S10.COMSOL simulation analysis of droplet bounce height on L-AAO@PFOTS surfaces with (a)d=0.15,s=0.15,(b)d=0.15,s=0.2 and (c)d=0.15,s=0.25.(d)Comparative analysis of COMSOL-simulated droplet bouncing heights recorded on L-Al and L-AAO@PFOTS surfaces.

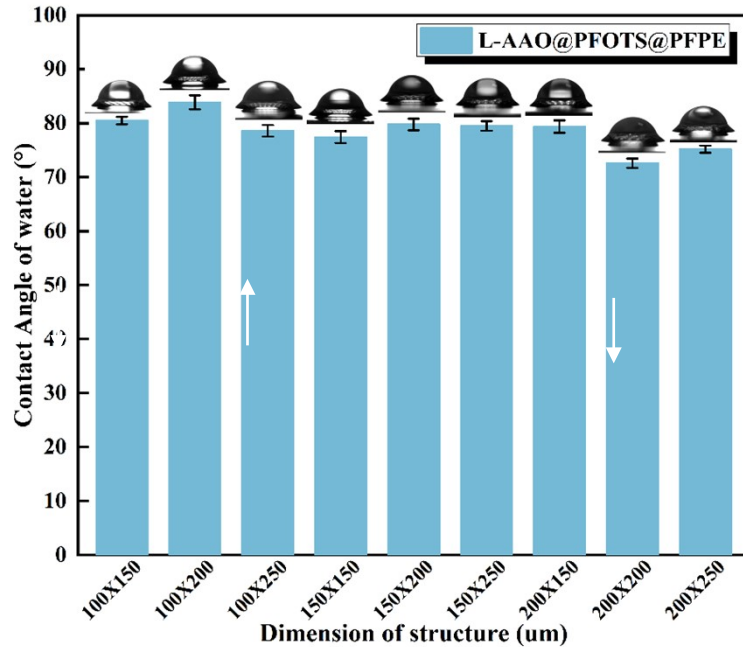


Fig.S11. Comparison of the contact angle of water on L-AAO@PFOTS@PFPE surfaces with different structural parameters.

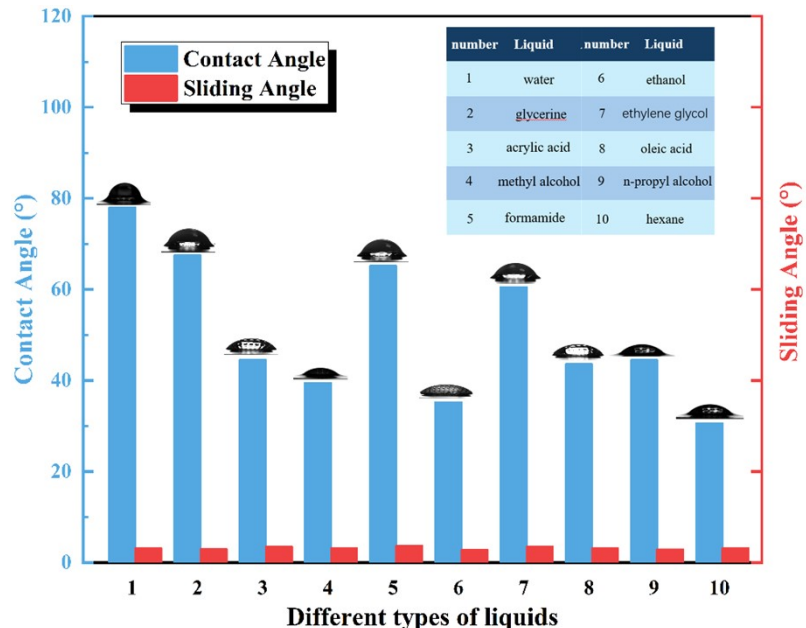


Fig.S12.Contact angle and sliding angle of different types of liquids on the L-AAO@PFOTS@PFPE suface.

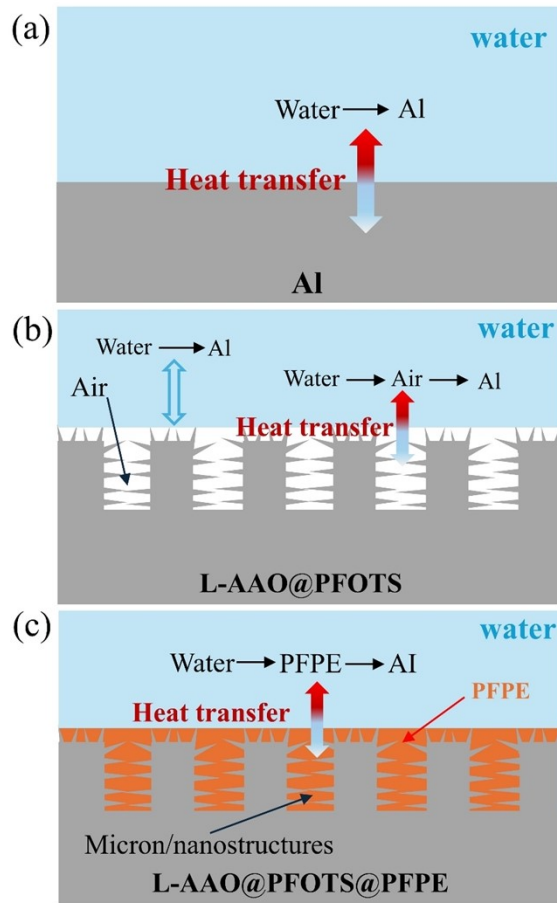


Fig.S13.Schematic of the ice formation and heat transfer process on (a)Al, (b)L-AAO@PFOTS, (c)and L-AAO@PFOTS@PFPE.

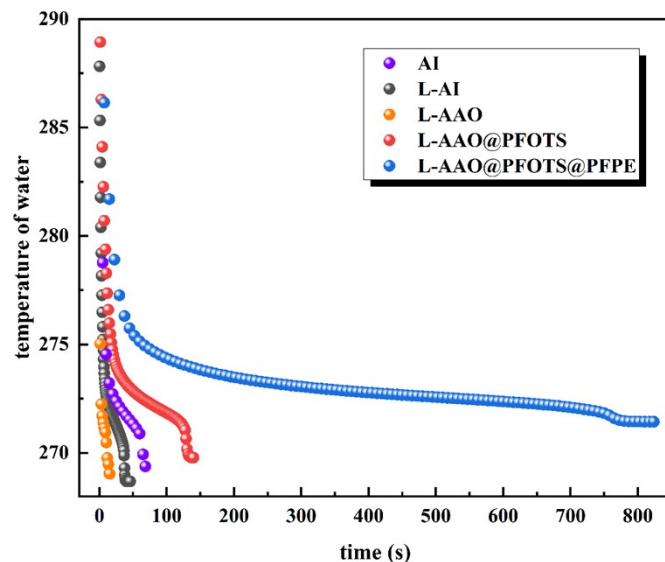


Fig.S14.Simulated data plots of icing rate and droplet average temperature for Al, L-Al, L-AAO, L-AAO@PFOTS, L-AAO@PFOTS@PFPE simulations.

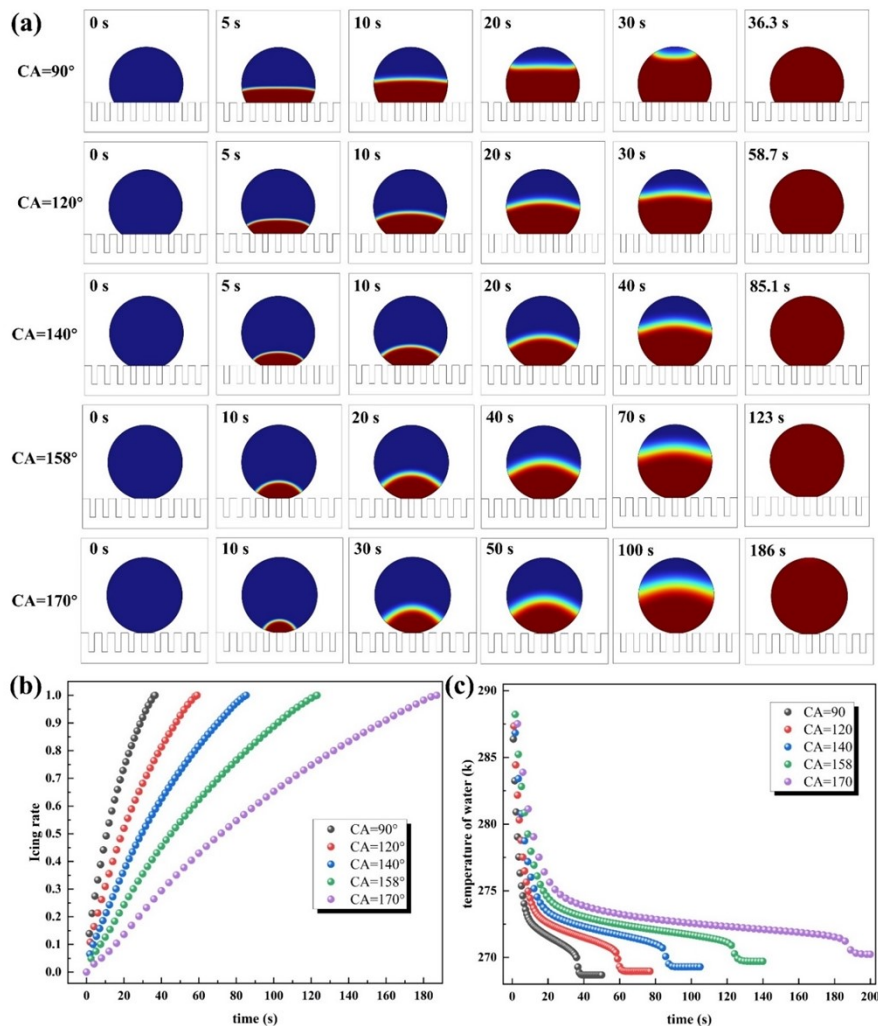


Fig.S15.The effect of different contact angle on the freezing time of the samples.

(a) Icing process ,(b)Icing rate and (c) Average temperature.

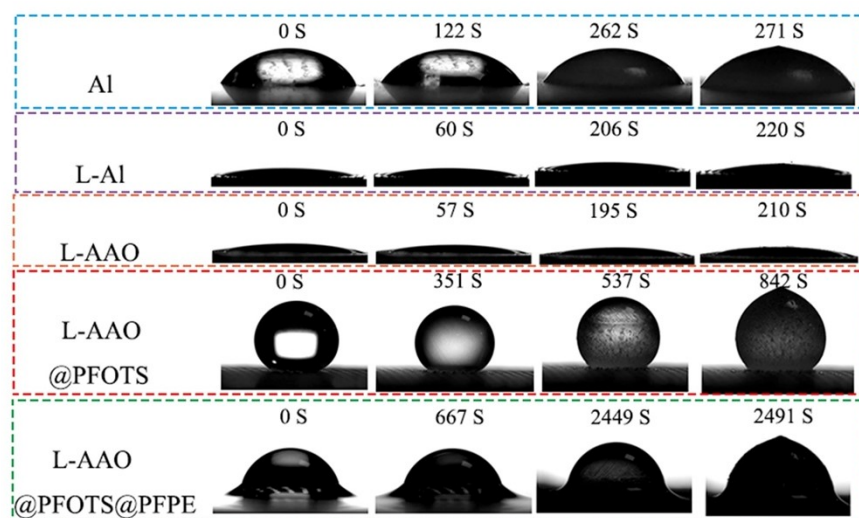


Fig.S16.Comparison of freezing time for droplets on Al, L-Al, L-AAO, L-AAO@PFOTS, and L-AAO@PFOTS@PFPE.

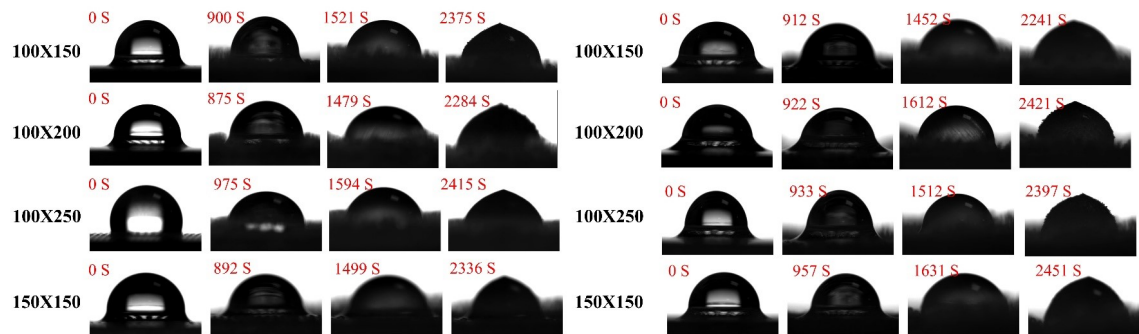


Fig.S17.Delayed icing process of L-AAO@PFOTS with different structural parameters

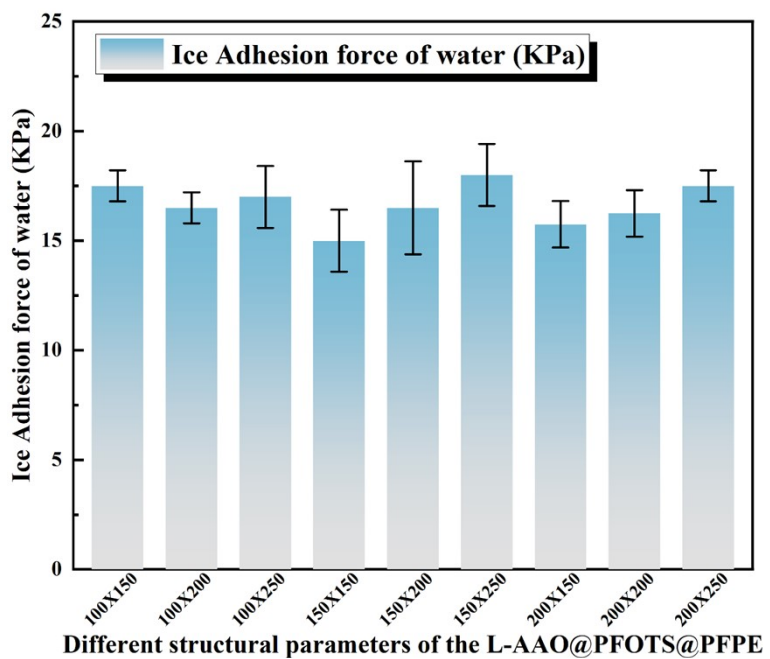


Fig.S18. Ice adhesion strength on L-AAO@PFOTS@PFPE surface with different structural parameters.

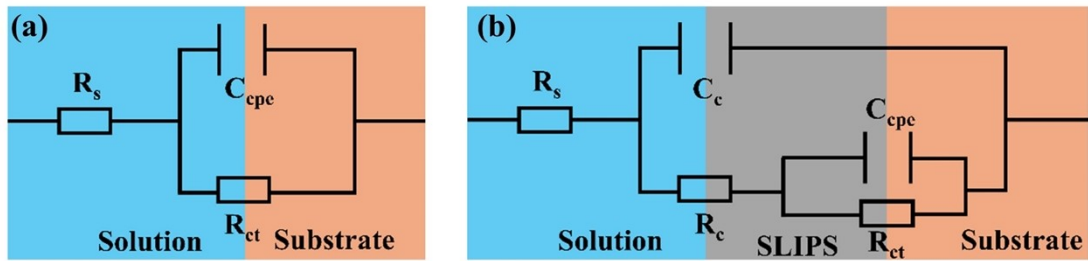


Fig.S19. The electrochemical equivalent circuit used to fit the EIS data of (a) bare Al and (b) L-AAO@PFOTS@PFPE samples.

TableS2.Fitting parameters obtained from EIS in different samples.

Sample	R_s ($\Omega \text{ cm}^2$)	C_c (F cm^2)	R_c ($\Omega \text{ cm}^2$)	R_{ct} ($\Omega \text{ cm}^2$)	C_{cpe} (F cm^2)
Al	41.75	3.98×10^{-5}	-	5.72×10^4	-
L-Al	27.17	5.14×10^{-5}	8.38×10^2	1.22×10^3	1.78×10^{-3}
L-AAO	35.9	1.25×10^{-5}	3.02×10^3	1.75×10^3	4.93×10^{-5}
L-AAO@PFOTS	57	1.21×10^{-11}	4.18×10^4	3.7×10^5	2.89×10^{-7}
L-AAO@PFOTS@PFPE	59	3.45×10^{-9}	3.45×10^5	2.1×10^6	1.76×10^{-7}

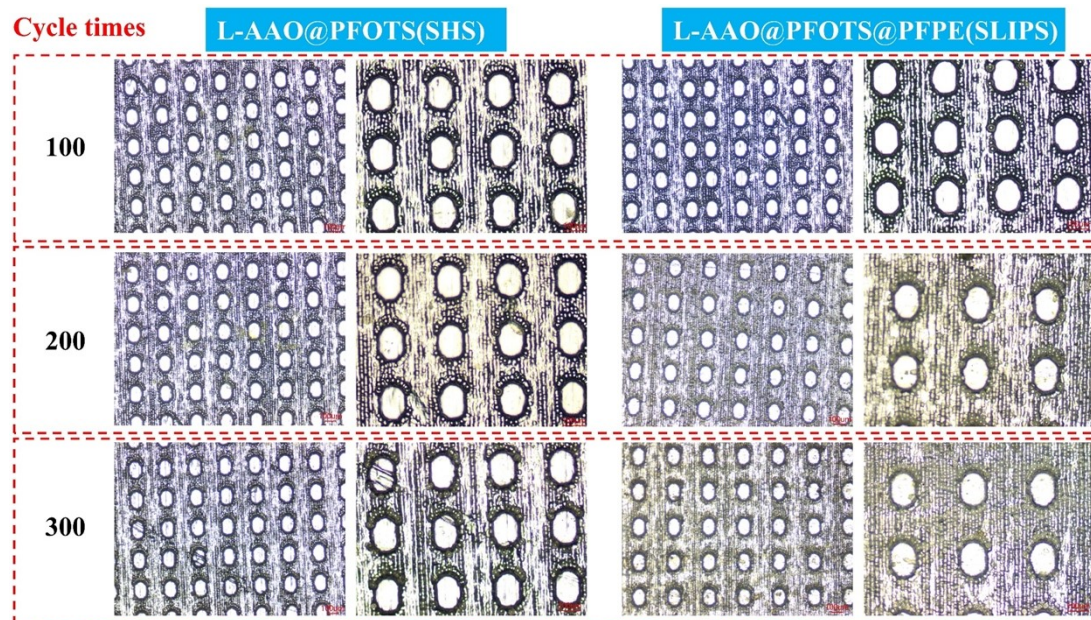


Fig.S20.Effect of friction wear cycles on the surface morphology of L-AAO@PFOTS and L-AAO@PFOTS@PFPE surface.

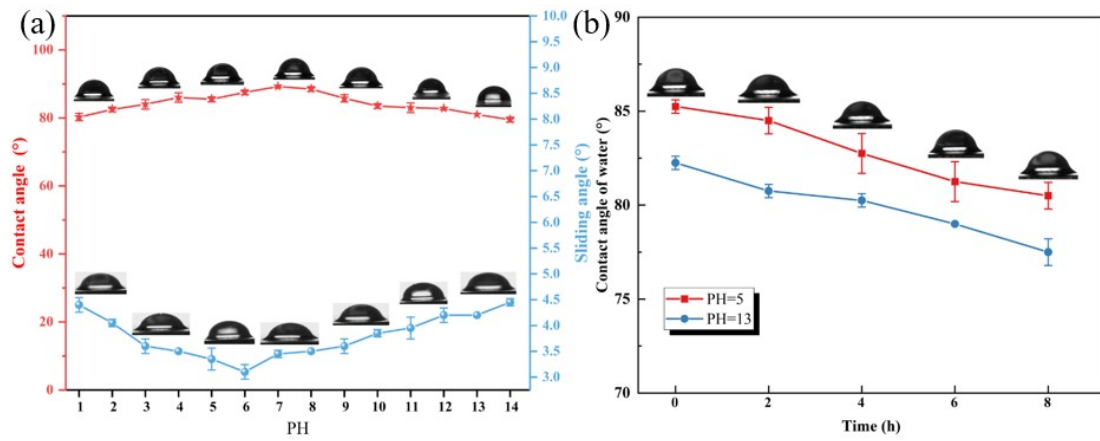


Fig.S21. (a) Characterization of contact angle (sliding angle) performance for droplets with different pH values on the super-slippery surface. (b) Changes in contact angle of the super-slippery surface after immersion in solutions with varying pH values (pH = 5 and 13) for different durations.